Available online at www.sciencedirect.com
SCIENCE DIRECT®
Talanta 67 (2005) 449–455
Talanta
www.elsevier.com/locate/talanta

A two-color-change, nanoparticle-based method for DNA detection

Y. Charles Cao, Rongchao Jin, C. Shad Thaxton, Chad A. Mirkin *

Department of Chemistry and Institute for Nanotechnology, Northwestern University, 2145 Sheridan Road, Evanston, IL 60208, USA

Abstract

Herein, we describe the detailed synthesis of Ag/Au core-shell nanoparticles, the surface-functionalization of these particles with thiolated oligonucleotides, and their subsequent use as probes for DNA detection. The Ag/Au core-shell nanoparticles retain the optical properties of the silver core and are easily functionalized with thiolated oligonucleotides due to the presence of the gold shell. As such, the Ag/Au core-shell nanoparticles have optical properties different from their pure gold counterparts and provide another "color" option for target DNA-directed colorimetric detection. Size-matched Ag/Au core-shell and pure gold nanoparticles perform nearly identically in DNA detection and melting experiments, but with distinct optical signatures. Based on this observation, we report the development of a two-color-change method for the detection and simultaneous validation of single-nucleotide polymorphisms in a DNA target using Ag/Au core-shell and pure gold nanoparticle probes.

Keywords: Two-color-change; Oligonucleotides; Detection; Core-shell; Nanoparticles

1. Introduction

Developing rapid DNA-detection methods is important for life science research and the clinical diagnosis of pathogenic and genetic diseases [1,2]. Current DNA assays are dominated by techniques that rely on target hybridization using fluorescent, radioactive, or chemiluminescent molecular probes [3,4]. Recently, gold nanoparticle probes (Au-NPs) heavily functionalized with thiolated oligonucleotides have emerged as an attractive alternative to molecular probes for nucleic acid detection [5–7]. Such probes have been used in both heterogeneous (e.g. microarrays) and homogeneous solution detection formats for the detection of short synthetic strands, [7,8] polymerase chain-reaction products, [9] and genomic DNA targets [10,11]. In the case of microarray-based detection, we have demonstrated the use of nanoparticle probes in scanometric, [5] SERS-based, [12,13] and light scattering based formats [14,15]. In many cases, these assays provide increased multiplexing capabilities, target selectivity, and sensitivity when compared to assays based upon molecular probes [12]. In the case of homogeneous formats, Au-NP probes have been used to develop simple colorimetric assays for nucleic acid targets with moderate sensitivity [7,8,15–17].

In a typical homogeneous assay, two sets of gold nanoparticle probes are prepared, each with a unique target-specific oligonucleotide. In the presence of complementary target strands, the Au-NP probes form target-assembled aggregates. Dissociation of these nanoparticle aggregates as a result of heating and duplex DNA melting occurs over a very narrow temperature range and is characterized by exceptionally sharp melting profiles; the full width at half-maximum (FWHM) for the first derivatives of these melting transitions can be is as low as 1 °C [8]. Sharp melting transitions allow one to differentiate perfectly complementary target strands from those with single nucleotide mismatches, [6,7] whereas the analogous assays based upon molecular fluorophores do not offer such selectivity [7]. The formation and dissociation of nanoparticle aggregates are accompanied by color changes from red to purple and from purple to red, respectively. Such color changes can be enhanced by spotting the test solution onto a reverse-phase thin-layer chromatography (TLC) plate, known as the "Northwestern spot test". On the plate, the color change provides a visual analysis of the state of hybridization. This spot test is moderately sensitive (100 pM), rapid, and very low cost [7,8].

* Corresponding author.
E-mail address: chadnano@northwestern.edu (C.A. Mirkin).

0039-9140/$ – see front matter © 2005 Elsevier B.V. All rights reserved.
doi:10.1016/j.talanta.2005.06.063

By using nanoparticles that consist of different compositions, one can monitor the hybridization state of two targets simultaneously due to the distinct optical signatures of each particle set. Specifically, Ag/Au core-shell nanoparticles can be used in an analogous spot test to provide a yellow-to-dark-brown color change in the presence of a complementary target [18]. Using pure gold and Ag/Au core-shell nanoparticle-probe systems, we have developed a new detection method for single-nucleotide-polymorphisms (SNPs). This new method relies on monitoring the two-color changes available through these two types of nanoparticle probes, leading to a dual method of identifying SNPs that is more reliable than the detection methods that are based upon a single color change. Herein, we describe the design and synthesis of Ag/Au core-shell and pure-gold-nanoparticle DNA probes with nearly identical melting profiles. We then demonstrate their use to differentiate a 30-mer target from its single-nucleotide-mutated counterpart.

2. Experimental

2.1. Chemicals

$AgNO_3$, $NaBH_4$, $HAuCl_4{\cdot}3H_2O$, and trisodium citrate were purchased from Aldrich Chemical Company. Bis(*p*-sulfonatophenyl)phenylphosphine (BSPP) was purchased from Strem Chemicals. Reagents required for oligonucleotide synthesis were purchased from Glen Research. TLC alumina gel RP 18 reverse-phase plates were purchased from Alltech Associates. Nanopure H_2O (18.1 MΩ), purified with a Barnstead Nanopure ultrapure water system, was used for all experiments. An Eppendorf 5415C centrifuge was used for centrifugation of nanoparticle solutions.

2.2. General methods

Electronic absorption spectra of the oligonucleotides were recorded using a Hewlett-Packard (HP) 8452a diode array spectrophotometer or Jasco V530 UV-vis spectrophotometer. High-performance liquid chromatography (HPLC) was performed using a HP series 1100 HPLC. Transmission electron microscopy (TEM) images of DNA-functionalized Au nanoparticles were obtained on a Hitachi 8100 transmission electron microscope. Samples were prepared by pipetting 5 μL of colloid solution onto a carbon-coated copper grid (200 mesh, Ted Pella). After the evaporation of solvent, the grid was dried overnight under vacuum. The TEM operating voltage was 200 kV, and the filament current was 10 μA. All of the images are bright-field images.

2.3. Synthesis of Au nanoparticles

Au particles (13 nm in diameter) were prepared by the citrate reduction of $HAuCl_4$. An aqueous solution of $HAuCl_4$ (1 mM, 250 mL) was brought to reflux while stirring whereupon 25 mL of a 38.8 mM trisodium-citrate solution was rapidly added. This led to a change in the color of the solution from pale yellow to dark red. After the color change, the solution was refluxed for an additional 5 min, allowed to cool to room temperature, and subsequently filtered through a Micron Separations Inc., 0.45 μm nylon filter. The resulting red solution of 13-nm-diameter gold particles exhibited a characteristic surface plasmon band at 518 nm.

2.4. Synthesis of Ag/Au core-shell nanoparticles

Core-shell nanoparticles were synthesized by using a two-step strategy. In the first step, Ag nanoparticles were prepared using literature methods [22]. The particles were then passivated with BSPP (0.3 mM), purified by centrifugation (collecting the primary fraction; ∼12 nm in diameter), and redispersed in Nanopure water. Second, gold shells were grown on the surface of the Ag nanoparticles (0.32 nmol of Ag particles in 100 mL of 0.3 mM sodium-citrate aqueous solution) by adding shell-growth precursor (i.e., simultaneously treating the Ag nanoparticle solution with $HAuCl_4$ and sodium borohydride via dropwise addition at 0 °C on the benchtop) [18]. The shell thickness is controlled by the amount of the added precursor; the more precursor added, the thicker the resulting shell. UV-vis spectrophotometry was used to monitor the shell thickness. When a desired shell thickness was achieved, the reaction was stopped, and 30 μmol of BSPP was added. The Ag/Au core-shell nanoparticles were then purified by centrifugation and redispersed in Nanopure water.

2.5. Synthesis of oligonucleotides

All of the oligonucleotides were synthesized on a 1 μmol scale using standard phosphoramidite chemistry on an automated synthesizer (Milligene Expedite) [19]. The 3′-propylthiol-capped oligonucleotides were prepared using 3′-Thiol-Modifier C3 S-S CPG solid supports. For the 5′-hexylthiol-capped oligonucleotides, the detritylated-oligonucleotide derivative on CPG support was first prepared on the synthesizer, followed by a manual synthesis procedure reported previously to couple the 5′-thiol moiety to the oligonucleotides using 5′-Thiol-Modifier C6 S-S phosphoramidite [7]. The oligonucleotides were cleaved from the CPG supports by soaking in concentrated NH_4OH for 16 h in a 55 °C oven and purified using HPLC as previously described [7]. After HPLC purification, the dimethoxytrityl (DMT) protecting group had to be removed from the 5′-termini of the target and 3′-propylthiol oligonucleotides by adding glacial acetic acid. DMT was extracted from the aqueous DNA solution using ethyl acetate (three times, 0.5 mL each). Finally, residual ethyl acetate was removed by purging the solution with N_2 for 10 min. The purified DNA (∼0.5 mL) was stored at −20 °C prior to use.

2.6. Functionalization of Au and Ag/Au nanoparticles

Before the 3′-alkylthiol modified DNA was used to functionalize the surfaces of the nanoparticles, the disulfide was reduced using dithiolthretol (DTT, 0.1 M) in phosphate buffer (0.17 M at pH 8) for 2 h. The 5′-alkylthiol DNA was deprotected with aqueous $AgNO_3$ (50 mM) for 20 min followed by treatment with DTT solution (10 mg/mL) for 5 min to remove excess $AgNO_3$. The resulting precipitate was removed by centrifugation. Aliquots of the deprotected DNA solution were purified through a desalting NAP-5 column (Sephadex G-25 medium, DNA grade, Pharmacia Biotech.).

Both Au and Ag/Au nanoparticles were functionalized by adding the deprotected thiolated oligonucleotides to the colloidal solutions (final concentration of oligonucleotides 2–3 μM). After ∼16 h, the colloidal solution was brought to 10 mM of phosphate (NaH_2PO_4/Na_2HPO_4) buffer. In a subsequent salt-aging process, the colloids were brought to a [NaCl] of 0.05 M by dropwise addition of 2 M NaCl solution and allowed to stand for 8 h, then 0.1 M for another 8 h, 0.2 M for another 8 h, and finally to 0.3 M NaCl. This process results in the most effective loading of oligonucleotides on the nanoparticle surfaces and has been studied in detail for the pure gold system [6]. To remove excess DNA, solutions were centrifuged in 1.5 mL Eppendorf tubes (Fisher Scientific), followed by removal of the supernatant to yield an oily precipitate. This precipitate was then washed with 0.3 M NaCl, pH 7, 10 mM phosphate buffer solution (for simplicity, designated as 0.3 M PBS below), recentrifuged, and redispersed in 0.3 M PBS. This washing procedure was repeated twice whereupon the colloid was resuspended in 0.01% azide, 0.3 M PBS, and stored at 4 °C [6].

2.7. Hybridization of nanoparticle probes with targets in the solution system

The molar concentrations of Au particle probes were measured by using UV-Vis spectroscopy [6]. Two sets of DNA-functionalized Au nanoparticles (probes a and b in 0.3 M PBS, 1.5 pmol of each for 13-nm Au particles were mixed at a 1:1 ratio), and target DNA (60 pmol) was added to the deep red solution. The total volume of the reaction mixture was adjusted to 1 mL using 0.3 M PBS. The solutions were frozen using dry ice, and then warmed to room temperature gradually. After ∼2 h, macroscopic nanoparticle aggregates formed, and the characteristic purple color was observed. Spotting 5 μL of the solution containing the aggregates onto a C_{18} reverse-phase TLC plate (spot test) yielded the expected blue spot [7].

2.8. Melting analyses

The melting analyses were carried out using a HP 8453 diode array spectrophotometer equipped with a HP 89090a Peltier temperature controller (Hewlett-Packard). The melting process was monitored by measuring the change in extinction at 260 nm or the λ_{max} for the nanoparticles (400 and 520 nm for Ag/Au core-shell and Au nanoparticles, respectively). The aggregate suspension was stirred continuously with a magnetic stir bar at 460 rpm as the solution temperature was increased from 20 to 70 °C at 0.5 °C intervals with a holding time of 1 min prior to each spectroscopic measurement. The data for the melting curve were processed by a linear insertion at 0.1 °C divisions. The first derivative generated from the melting curves using the instrument software was used to determine the T_m and sharpness as measured by the full width at half-maximum [6].

3. Results and discussion

3.1. Synthesis and stability of Ag/Au core-shell nanoparticles

Ag/Au core-shell nanoparticles were made using a two-step approach. Ag nanoparticles were sythesized in the first step, followed by shell growth in the second step. To obtain particles with ideal optical properties, in the gold-shell-growth step, one must avoid the formation of an alloy of gold and silver, the nucleation of gold clusters, and size-distribution broadening during shell growth. Gold atoms have a radius very close to that of silver atoms, and the lattice mismatch between gold and silver crystals is nearly zero [20]. The near-zero lattice mismatch promotes gold shell growth on silver particles. However, under some conditions, [21] it allows Au and Ag to alloy due to the diffusion of gold atoms into the silver nanoparticles, a thermally activated process. Until recently, unintentional alloying was a major reason for difficulties in the synthesis of Au/Ag core-shell nanoparticles [21]. To avoid alloying, we chose to reduce the temperature at which shell growth was carried out (∼ 0 °C). In addition, BSPP was added into the solution to further stabilize the gold shell during growth. At room temperature, BSPP-passivated Ag/Au core-shell nanoparticles are stable for more than one month without substantial alloy formation as evidenced by no substantive change in the UV-vis spectrum of the colloid over this time frame. In a typical synthesis, gold shells were grown onto the surface of the Ag nanoparticles by simultaneously treating them with $HAuCl_4$ and sodium borohydride via dropwise addition. The simultaneous dropwise addition of dilute Au precursors inhibits the formation of gold-cluster nucleation sites by keeping the concentration of these gold-forming reagents low. However, if the concentration of the gold-forming reagents is too low, size-distribution broadening of the particle occurs due to Ostwald ripening. We have determined that a concentration of ∼2 μM for the gold-forming reagents is optimal for gold shell growth (concentration range studied: 0.20–20 μM).

Core-shell particles with a one-monolayer thick gold shell exhibit an extinction spectrum that is very similar to that for citrate-stabilized, pure-Ag particles [22]. The surface plas-

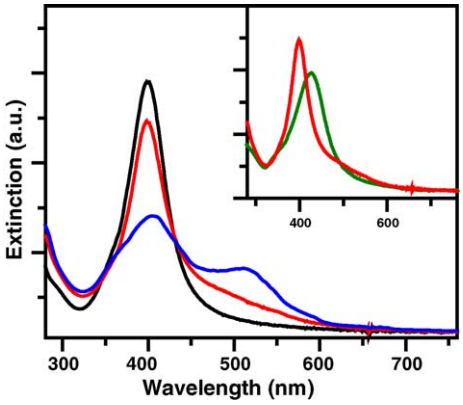

Fig. 1. UV-vis spectra of Ag core (black) and Ag/Au core-shell with a shell thickness of one monolayer (red) and two monolayers (blue). The inset shows Ag/Au core-shell with a shell thickness of one monolayer (red) and Ag/Au alloy nanoparticles.

mon band of the Ag remains at the same wavelength but is dampened by about 10%, and the gold plasmon band is observed as a weak feature at 500 nm. However, as the gold shell is grown to approximately two monolayers, the silver surface plasmon band is dampened by more than 50% at the same wavelength, and the gold plasmon band exhibits a more intense peak at 514 nm (Fig. 1). These spectral features provide a means of following the gold shell growth process and characterizing the resulting core-shell structures. By using energy dispersive X-ray spectroscopy (EDS), the ratio between Ag and Au was also followed to quantify and monitor the growth of the Au shell. It should be noted that by using different procedures, others have prepared gold-coated silver nanoparticles, but those procedures lead to Ag/Au alloys [21]. The extinction spectra of such particles exhibit characteristic red shifting and broadening of the plasmon resonance. Moreover, if one intentionally makes a solution of alloyed Ag/Au particles with the same Ag/Au atomic ratio, they can be easily distinguished from core-shell particles with comparable Ag/Au ratios [21,23]. Indeed, the core-shell Ag/Au nanoparticles prepared in this work retain the optical properties of the core with no observed red-shifting of the Ag plasmon band (Fig. 1). As Ag/Au core-shell particles retain the spectral features of silver when coated with a single monolayer, these were chosen for biological labeling.

Surface modification of the core-shell nanoparticles with alkanethiol-capped oligonucleotides was accomplished using a procedure nearly identical to the one used for 13-nm gold particles. The oligonucleotide-modified particles exhibit the stability of their pure-gold counterparts and can be suspended in 1 M NaCl solutions indefinitely. This is important for use in DNA detection assays since such reactions are facilitated in solutions with elevated salt-concentrations [6,7]. More interestingly, alkanethiol-capped-oligonucleotide-functionalized Ag/Au core-shell nanoparticles exhibit a higher stability than the core-shell particles passivated only by BSPP, which are stable for up to six months at room temperature without Ag/Au-alloy formation. In part, this result can be explained by the increased affinity of alkanethiols to Au as compared with BSPP [20].

3.2. *Two-color-change labeling for DNA detection*

We chose a 30-mer DNA target to study the feasibility of establishing a two-color-labeling assay using Ag/Au core-shell and pure-gold nanoparticles (Fig. 2A). Oligonucleotide probes a and b were functionalized on both Ag/Au core-shell nanoparticles and pure-gold nanoparticles (Fig. 2B and C,

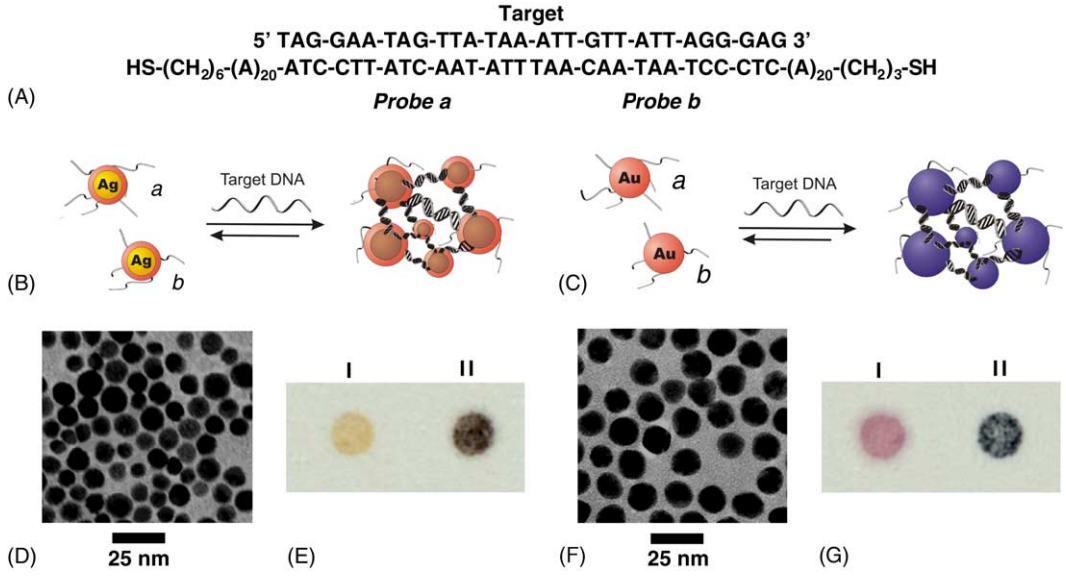

Fig. 2. (A) Mercaptoalkyl-capped-oligonuleotide probes and oligonucleotide target. (B) Scheme for Ag/Au core-shell nanoparticle-based detection; (C) Scheme for pure gold nanoparticle-based detection; (D) TEM image of Au/Ag nanoparticles; (E) 12.6 nm Ag/Au nanoparticle probes (I) without target, (II) with target at room temperature; (F) TEM image of gold nanoparticles; (E) 13.0-nm gold-nanoparticle probes (I) without target, (II) with target at room temperature.

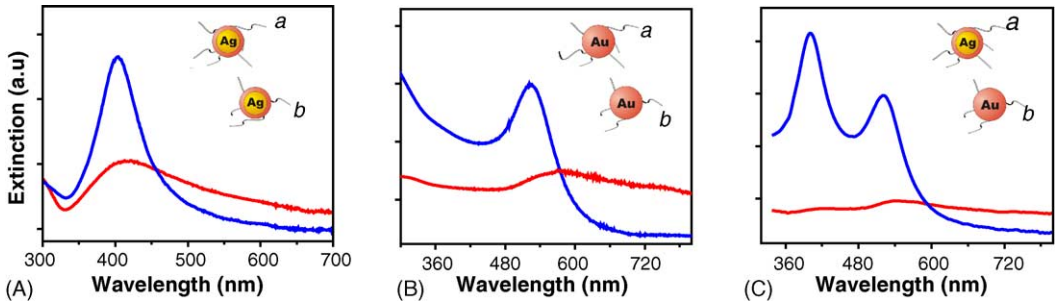

Fig. 3. UV-vis spectra of dispersed oligonucleotide-modified nanoparticles (blue) and aggregated (red) oligonucleotide-modified nanoparticles formed via hybridization: (A) Ag/Au core-shell; (B) pure gold particles; and (C) Hybrid Ag/Au core-shell and pure-gold particles.

respectively). In the presence of the complementary target, the nanoparticles form aggregate structures with a concomitant darkening of the solution. However, no distinct color change is observable by the naked eye for Ag/Au core-shell nanoparticles, while a red-to-purple change is observed for pure-gold nanoparticles. In order to enhance the color change associated with target-induced particle aggregation, the sample was spotted onto a C_{18} reverse-phase alumina TLC plate. With the core-shell particles, a distinct yellow-to-dark-brown color change is observed upon particle assembly in the presence of the complementary target (Fig. 2E-I and E-II). As such, the core-shell probes provide a route to a second colorimetric change distinct from the pure gold system (Fig. 2C). The color change is due to a red-shift and dampening of the plasmon resonance of the core-shell particles (or gold particles) upon DNA-induced aggregation (Fig. 3A and B). Particle aggregates formed from the cross-linking of Ag/Au core-shell with pure-gold nanoparticles did not lead to an additional color change when spotted onto a C_{18} reverse-phase alumina TLC plate. However, such hybrid-particle-aggregate systems were distinguishable using UV-vis spectroscopy (Fig. 3C).

The particles within the aggregate structures can be dispersed by heating the aggregates above the "melting temperature" (T_m) of the duplex DNA interconnects. The Ag/Au-core-shell-nanoparticle aggregates exhibit melting profiles nearly identical to the pure-gold-nanoparticle aggregates in solutions with different salt concentrations (Fig. 4). The full width at half-maximum for the first derivatives of these melting transitions is less than 3 °C. The deviation in melting point between these two nanoparticle systems is less than 0.3 °C under identical conditions. Such nearly-identical melting profiles for these two nanoparticle systems, in part, originate from the fact that these nanoparticles have similar diameters (12.6 nm for Ag/Au core-shell nanoparticles, and 13.0 nm for Au nanoparticles and presumably similar degrees of oligonucleotide surface coverage, (Fig. 2D and F) [6]. Taken together, these results show that Ag/Au core-shell and pure-gold nanoparticles are near identical labels for hybridization-based DNA detection, but impart different color changes. This identical labeling function is a prerequisite for using Ag/Au and pure-gold nanoparticles in parallel-detection experiments.

3.3. SNP analysis based on two-color-change labeling

The two target strands (i.e., wild-type and mutant) are 30-mers that span the wild-type and single nucleotide mutation in the beta-globin gene that results in sickle-cell anemia. The oligonucleotide probes were designed accordingly (Fig. 5A). Oligonucleotides perfectly complementary to the normal target were used to modify the gold particles (13.0 nm in diameter), and those perfectly complementary to the mutation target were used to functionalize the Ag/Au core-shell nanoparticles (12.6 nm in diameter).

Two experiments were carried out to evaluate the suitability of a two-color-change labeling system for SNP analysis. In the first experiment, the normal target was added to solutions containing the pure-gold and Ag/Au core-shell nanoparticle probe systems, respectively. The particle aggregates in

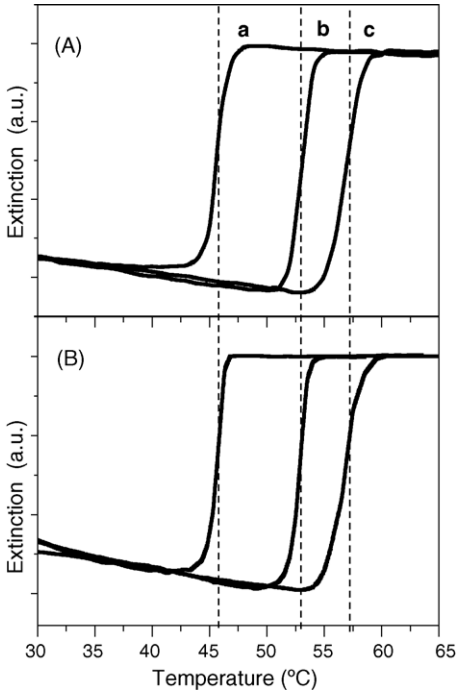

Fig. 4. Thermal denaturation curves of aggregates formed from hybridized oligonucleotide-modified particles in PBS buffer solutions: (A) Ag/Au core-shell and (B) pure-gold nanoparticles (a, 0.1 M NaCl; b, 0.3 M NaCl; and c, 0.5 M NaCl).

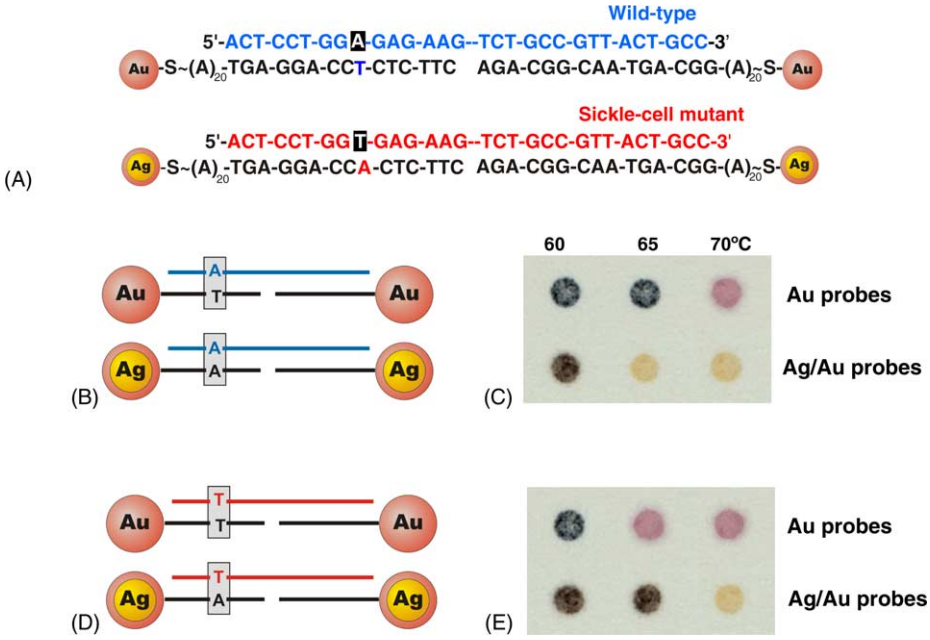

Fig. 5. (A) Mercaptoalkyl-oligonuleotide-modified Ag/Au core-shell and pure-gold particles, and their oligonucleotide targets. (B) Scheme for the parallel-detection experiments in the presence of the wild-type targets. (C) Spot-test result in the presence of the wild-type targets. (D) Scheme for the parallel-detection experiments in the presence of the mutant targets. (E) Spot-test result in the presence of the mutant targets.

the pure-gold system showed a higher melting temperature compared to the core-shell-particle system (Fig. 5B and C). Here, the wild-type target is perfectly complementary to the gold probes, but there is a single nucleotide mismatch with the core-shell probes (Fig. 5A). In the second experiment, the mutant target was added to the same two probe systems. The opposite result was obtained. The particle aggregates in the core-shell-particle system exhibit a higher melting point than that of the aggregates formed in the pure-gold probe system (Fig. 5D and E). The results from these two experiments show that one can easily distinguish the SNP targets according to the different patterns in the TLC spot test. In addition, the parallel-detection experiments based on the two-color changes reference one another, eliminating potential errors caused by experimental defects such as deviations in temperature control and salt concentrations in the hybridization solutions.

4. Conclusions

This work provides a number of important observations and conclusions. First, it provides a refined method for making Ag/Au core-shell nanoparticles with the optical properties of silver but the chemical stability of gold. The conditions for gold-shell growth were optimized to minimize alloy formation, nucleation of gold particles, and the size-distribution broadening of the core-shell particles during growth. Second, Ag/Au core-shell and pure-gold nanoparticles function nearly identically as DNA-hybridization labels, but with different optical properties. Third, Ag/Au core-shell and pure-gold nanoparticles can be used to establish a new two-color-change-based method for SNP analysis. The two-color-change-based detection provides a convenient cross-check and an assay control that allows for more accurate readout when compared to the single-color-change methods.

Acknowledgments

C.A.M. acknowledges the AFOSR, DARPA, NIH, and NSF for support of this research.

References

[1] S. Razin, Mol. Cell. Probes 8 (1994) 497.
[2] J.G. Hacia, L.C. Brody, M.S. Chee, S.P. Fodor, F.S. Collins, Nat. Genet. 14 (1996) 441.
[3] B.D. Hames, S.J. Higgins (Eds.), Gene Probes 1, IRL Press, New York, 1995.
[4] S. Tyagi, F.R. Kramer, Nat. Biotechnol. 14 (1996) 303.
[5] T.A. Taton, R.L. Letsinger, C.A. Mirkin, Science 289 (1999) 1757.
[6] R. Jin, G. Wu, Z. Li, C.A. Mirkin, G.C. Schatz, J. Am. Chem. Soc. 126 (2003) 1643.
[7] J.J. Storhoff, R. Elghanian, R.C. Mucic, C.A. Mirkin, R.L. Letsinger, J. Am. Chem. Soc. 120 (1998) 1959.
[8] R. Elghanian, J.J. Storhoff, R.C. Mucic, R.L. Letsinger, C.A. Mirkin, Science 277 (1997) 1078.
[9] J.J. Storhoff, S.S. Marla, V. Garimella, C.A. Mirkin, Microarray Technol. Appl. (2004) 147.
[10] J.J. Storhoff, S.S. Marla, P. Bao, S. Hagenow, H. Mehta, A. Lucas, V. Garimella, T. Patno, W. Buckingham, W. Cork, U.R. Muller, Biosci. Bioelec. 19 (2004) 875.
[11] Y.P. Bao, M. Huber, T.F. Wei, S.S. Marla, J.J. Storhoff, U.R. Muller, Nucl. Acids Res. 33 (2005) e15.

[12] Y.C. Cao, R. Jin, C.A. Mirkin, Science 297 (2002) 1536.
[13] Y.C. Cao, R.C. Jin, J.M. Nam, C.S. Thaxton, C.A. Mirkin, J. Am. Chem. Soc. 125 (2003) 14676.
[14] T.A. Taton, G. Lu, C.A. Mirkin, J. Am. Chem. Soc. 123 (2001) 5164.
[15] J.J. Storhoff, A.D. Lucas, V. Garimella, Y.P. Bao, U.R. Muller, Nat. Biotech. 22 (2004) 883.
[16] K. Sato, K. Hosokawa, M. Maeda, J. Am. Chem. Soc. 125 (2003) 8102.
[17] R. Chakrabarti, A.M. Klibanov, J. Am. Chem. Soc. 125 (2003) 12531.
[18] Y. Cao, R. Jin, C.A. Mirkin, J. Am. Chem. Soc. 123 (2001) 7961.
[19] F. Eckstein (Ed.), Oligonucleotides and Analogues, first ed., Oxford University Press, New York, 1991.
[20] D.R. Lide (Ed.), Handbook of Chemistry and Physics, CRC Press, Boca Raton, 1992.
[21] P. Mulvaney, M. Giersig, A. Henglein, J. Phys. Chem. 97 (1993) 7061.
[22] L. Rivas, S. Sanchez-Cortes, J.V. Garcia-Ramos, G. Morcillo, Langmuir 16 (2000) 9722.
[23] S. Link, Z.L. Wang, M.A. El-Sayed, J. Phys. Chem. B 103 (1999) 3529.